Charge-transfer interactions induce surface dependent conformational changes in apolipoprotein biocorona

Achyut J. Raghavendra
Laboratory of Nano-Biophysics, Clemson Nanomaterials Center, Department of Physics and Astronomy, Clemson University, Clemson, South Carolina 29634

Nasser Alsaleh and Jared M. Brown[a]
Department of Pharmaceutical Sciences, Skaggs School of Pharmacy and Pharmaceutical Science, University of Colorado-Anschutz Medical Campus, Aurora, Colorado 80045

Ramakrishna Podila[a]
Laboratory of Nano-Biophysics, Clemson Nanomaterials Center, Department of Physics and Astronomy, Clemson University, Clemson, South Carolina 29634 and Center for Optical Materials Science and Engineering Technologies (COMSET), Clemson, South Carolina 29625

Upon introduction into a biological system, engineered nanomaterials (ENMs) rapidly associate with a variety of biomolecules such as proteins and lipids to form a biocorona. The presence of "biocorona" influences nano–bio interactions considerably, and could ultimately result in altered biological responses. Apolipoprotein A-I (ApoA-I), the major constituent of high-density lipoprotein (HDL), is one of the most prevalent proteins found in ENM-biocorona irrespective of ENM nature, size, and shape. Given the importance of ApoA-I in HDL and cholesterol transport, it is necessary to understand the mechanisms of ApoA-I adsorption and the associated structural changes for assessing consequences of ENM exposure. Here, the authors used a comprehensive array of microscopic and spectroscopic tools to elucidate the interactions between ApoA-I and 100 nm Ag nanoparticles (AgNPs) with four different surface functional groups. The authors found that the protein adsorption and secondary structural changes are highly dependent on the surface functionality. Our electrochemical studies provided new evidence for charge transfer interactions that influence ApoA-I unfolding. While the unfolding of ApoA-I on AgNPs did not significantly change their uptake and short-term cytotoxicity, the authors observed that it strongly altered the ability of only some AgNPs to generate of reactive oxygen species. Our results shed new light on the importance of surface functionality and charge transfer interactions in biocorona formation.
© 2017 American Vacuum Society. [http://dx.doi.org/10.1116/1.4977064]

I. INTRODUCTION

The sustainable implementation of engineered nanomaterials (ENMs) in biological applications, such as drug delivery and imaging, requires a comprehensive understanding of complex transformations and interactions at the nano–bio interface.[1–4] ENMs are known to rapidly associate with a variety of biomolecules (e.g., proteins, amino acids, and lipids) in any biological milieu to form a biocorona on their surfaces.[5–12] The presence of biocorona on ENMs imparts a new distinctive interactive surface, which ultimately determines the biological implications and fate of ENMs. Previous studies showed that ENM-biocorona (ENM-BC) leads to various physiological and pathological changes, including protein aggregation, blood coagulation, and complement activation.[5–12]

Although many physicochemical characteristics of ENM have been reported to influence ENM-BC, it is not yet clear what combination of these properties could be used to predict ENM-BC formation and evolution.[13,14] The composition of ENM-BC is known to strongly depend on ENM size and surface charge.[5,6,9–11,15–21] Larger ENMs exhibit a preferential adsorption of higher molecular weight proteins whereas lower molecular weight proteins accumulate more on the surface of smaller ENMs. On the other hand, surface charge is expected to be a key factor in determining protein structural changes.[9,10,12–15,21] The interactions between ENM surface and proteins could disrupt the structural integrity of proteins in ENM-BC and impact their function or elicit adverse immune responses. The surface coatings or functional groups are physically and chemically more active relative to the core of ENM. For instance, citrate groups adsorbed on the surface of Ag nanoparticles (AgNPs) are negatively charged and provide electrostatic repulsion needed to prevent AgNP aggregation. Any oppositely charged biomolecules (compared to surface functional groups on ENM) experience a natural electrostatic attraction to adsorb on ENM surface. Proteins with a stronger affinity to the ENM core can quickly displace the initially present functional groups and be irreversibly immobilized on ENM surface by partial or complete denaturation.[13,15,22] A combination of many factors including van der Waals forces, hydrogen bridges, charge transfer and other hydrophobic

[a]Authors to whom correspondence should be addressed; electronic addresses: jared.brown@ucdenver.edu; rpodila@g.clemson.edu

interactions are known to drive protein denaturation.[23–26] Such factors naturally depend upon ENM physicochemical properties. It is imperative to deconvolute the influence of different physicochemical properties (e.g., surface, charge, and size) and understand how they differ from each other in influencing protein adsorption and denaturation in ENM-BC.

Here, we experimentally investigated the influence of AgNP surface charges on adsorption and denaturation of apolipoprotein A-I (ApoA-I). Considering that ApoA-I is one of the most abundant proteins in AgNP-BC irrespective of AgNP size,[20] its adsorption on AgNPs with different surface coatings could provide new insights into the role of surface charges in ENM-BC. ApoA-I is the major protein component of high-density lipoprotein. It adopts a shape similar to a horseshoe of dimensions $12.5 \times 8 \times 4$ nm with high α-helix content.[27–31] The helices in ApoA-I are predicted to be amphipathic, with the hydrophobic (/hydrophilic) face mediating lipid (/aqueous) interactions. The thermodynamic drive to minimize the aqueous exposure of the hydrophobic residues is one of the major factors in ApoA-I adsorption on AgNPs.[32–36] Our light scattering and surface charge studies on 100 nm AgNPs (with four different functional groups) revealed that the binding of ApoA-I on AgNPs is sensitive to their surface charge and functionality. While ApoA-I exhibited strong affinity for both positively and negatively charged AgNPs, its secondary structure exhibited more pronounced changes for two surface functionalities, viz., lipoic acid and branched polyethylenimine (bPEI). In this article, we explain the observed secondary structural changes in terms of the electronic charge transfer, gleaned from electrochemical cyclic voltammetry (CV) experiments, between ApoA-I and functionalized AgNPs. Finally, the displacement of positively charged bPEI by ApoA-I and the structural changes of ApoA-I on AgNP-lipoic acid were found to induce a significant increase in their ability to generate reactive oxygen species (ROS). Our results provide new insights into the role of AgNPs surface charge in ENM-BC formation and its influence on bioresponse.

II. EXPERIMENT

Aqueous solution of AgNPs (100 nm, NanoXact, Nanocomposix) with citrate, polyvinylpyrrolidone (PVP), bPEI, and lipoic acid as capping agents was purchased. ApoA-I from human plasma (MW = 28.3 kDa) was purchased from Sigma–Aldrich. Different ApoA-I concentrations (0–4 g/l) were considered with AgNPs (5.4 mg/l) in deionized (DI) water to study hydrodynamic size and zeta potential using Zetasizer Nano ZS90 (Malvern Instruments). AgNPs were incubated with ApoA-I at $4\,^{\circ}C$ overnight to allow the formation of ApoA-I biocorona. For transmission electron microscopy (TEM) characterization of the corona formation, AgNPs with ApoA-I biocorona were stained with 0.1% osmium tetroxide (OsO_4) (diluted from 2% OsO_4—EMS Cat. 19152 with DI water) by incubating for 30 min. The samples were washed with DI water to remove any unbound OsO_4. Suspensions of AgNPs were bath sonicated for 5 min, before drop casted on 400 mesh Cu grid to air dry

overnight, and TEM images were acquired using a Hitachi H-7600 microscope. The resulting TEM images were false-colored using Photoshop (Adobe, San Jose, CA) where red, green, gray, and purple indicate citrate, PVP, bPEI, and lipoic acid coatings, respectively, on AgNPs.

Electrochemical studies were performed using a Gamry reference 3000 electrochemical system. CV measurements were obtained in a three-electrode setup with Ag/AgCl as the reference electrode, platinum wire as the auxillary/counter electrode, and AgNPs as the working electrode. We used ApoA-I solution as the electrolyte to study charge transfer. It should be noted that we used concentration ranges based on the physiological levels of ApoA-I ($\sim$1–1.3 g/l) for electrochemical studies to avoid high current values that could result in artifacts in charge transfer measurements.

Circular dichroism (CD) measurements were performed using Jasco spectropolarimeter (J-810) to analyze secondary structures of ApoA-I after the biocorona formation on AgNPs. Samples were prepared for CD analysis with suspensions of AgNPs and ApoA-I corresponding to molar ratio of 1:600 and incubated at $40\,^{\circ}C$ for 8 h. The CD spectra were measured at room temperature with wavelength range from 200 to 300 nm for all the samples at a scan speed of 50 nm/min. Background correction was applied with pure AgNP suspension.

ROS were evaluated using dichlorofluorescein (DCF) assay via flow cytometry. We utilized RAW 264.7, and macrophage mouse cell line was obtained from the American Type Culture Collection. Cells were cultured at $37\,^{\circ}C$ and 5% CO_2 in Dulbecco's modified eagle medium (DMEM) containing 10% heat-deactivated fetal bovine serum and 1.0% penicillin–streptomycin. RAW 264.7 cells were grown to 90% confluency. Cells were washed two times, media was replaced with unsupplemented DMEM medium, and then, the cells were exposed to 30 mg/l of AgNPs (with different coatings) for 1 h or 500 μM (17 mg/l) H_2O_2 for 30 min as a positive control. Then, the cells were washed twice with ice-cold phosphate-buffered saline (PBS) and then resuspended in 5 μM CM-H2DCFDA (Invitrogen)-containing PBS for 30 min at dark at $37\,^{\circ}C$. Ten thousand events were measured by Accuri[TM] C6 flow cytometry (BD Biosciences). Samples were kept on ice during reading at flow cytometry. All experiments were performed at least from three individual batches of cells.

Cell viability was assessed using 3-(4,5-dimethylthiazol-2-yl)-5-(3-carboxymethoxyphenyl)-2-(4-sulfophenyl)-2H-tetrazolium (inner salt; MTS) according to the manufacturer's instructions (Promega, Madison, WI). Briefly, RAW 264.7 cells were grown to 90% confluency in 96-well plates and were exposed to AgNPs in a serum-free DMEM/F12 HyClone GE media (Logan, UT) for 1 h. Then, cells were centrifuged (to bring nanoparticles to the bottom of wells), and supernatants were transferred to new plates and read at 490 nm (BioTek Synergy HT, BioTek, Winooski, VT).

III. RESULTS AND DISCUSSION

As shown in Fig. 1, TEM images confirmed that all four types of AgNPs (citrate, PVP, bPEI, and lipoic acid coated)
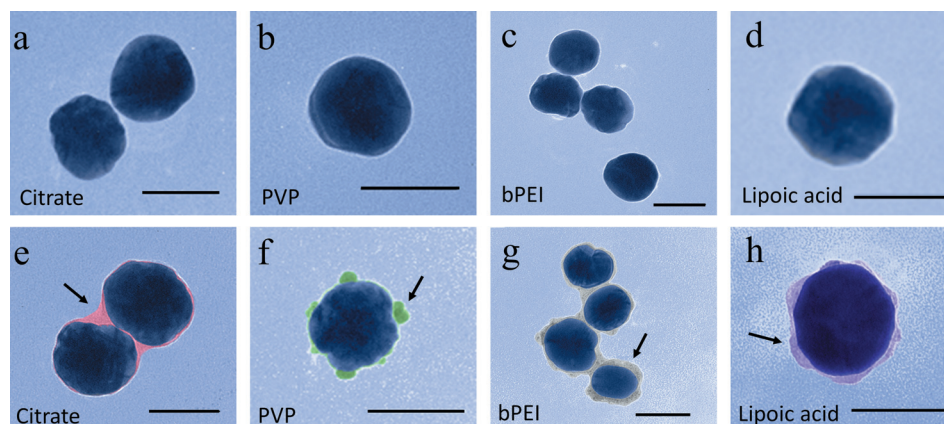
FIG. 1. Transmission electron micrographs showing as-purchased Ag NPs (a)–(d) with citrate, PVP, bPEI, and lipoic acid coatings, respectively. The presence of biocorona [see arrows in (e)–(h)] upon incubation with ApoA-I was assessed using OsO_4 staining as shown in (e)–(h). Scale bar is 100 nm.

are spherical in shape with a similar size of ∼100 nm in their dehydrated state. ApoA-I appeared to nonuniformly adsorb on to AgNPs [Figs. 1(e)–1(h)] with strong preference for rough edges (see Figs. 1(f) and 1(h) and supplementary Figs. S1–S4, Ref. 43). Given the small size of ApoA-I protein (hydrodynamic size ∼8 nm) relative to 100 nm AgNPs, the corona possibly consisted of multiple ApoA-I layers. In some cases, ApoA-I was found to envelop AgNP aggregates in the dehydrated state under TEM similar to previous observations[37] (Figs. S1–S4, Ref. 43).

Although all AgNPs have the same size in their dehydrated size (as evidenced by TEM), we found that their hydrodynamic sizes (S_{HD}) differed from each other in the following order: bPEI (∼135 nm) > PVP (∼120 nm) > lipoic acid (∼108 nm) > citrate (∼100 nm). This trend is expected based on the size of the surface coating molecules where polymers (bPEI and PVP) are significantly larger than the

smaller citrate and lipoic acid groups. The difference in the surface coatings was also evident from their zeta potential (ζ) measurements where bPEI is positively charged with a relative low $\zeta \sim 8.89$ mV while citrate ($\zeta \sim -39$ mV), PVP ($\zeta \sim -37$ mV), and liopic acid ($\zeta \sim -28$ mV) exhibited larger negative values. Based on the zeta potential measurements, negatively charged ApoA-I [($\zeta \sim -30$ to 36 mV (Ref. 37)] is expected to display strong electrostatic attraction toward bPEI coated AgNPs and possibly experience some repulsion from other negatively charged AgNPs.

We studied the evolution of S_{HD} and ζ of AgNPs in the presence of ApoA-I [Figs. 2(a) and 2(b)]. In the case of bPEI, ζ decreased rapidly and changed from a positive to negative value in the presence of ApoA-I. Indeed, ζ values at higher ApoA-I concentrations (∼−24 mV) suggest that ApoA-I stabilized AgNPs better than bPEI. A concomitant decrease in S_{HD} of AgNP-bPEI suggested that ApoA-I has
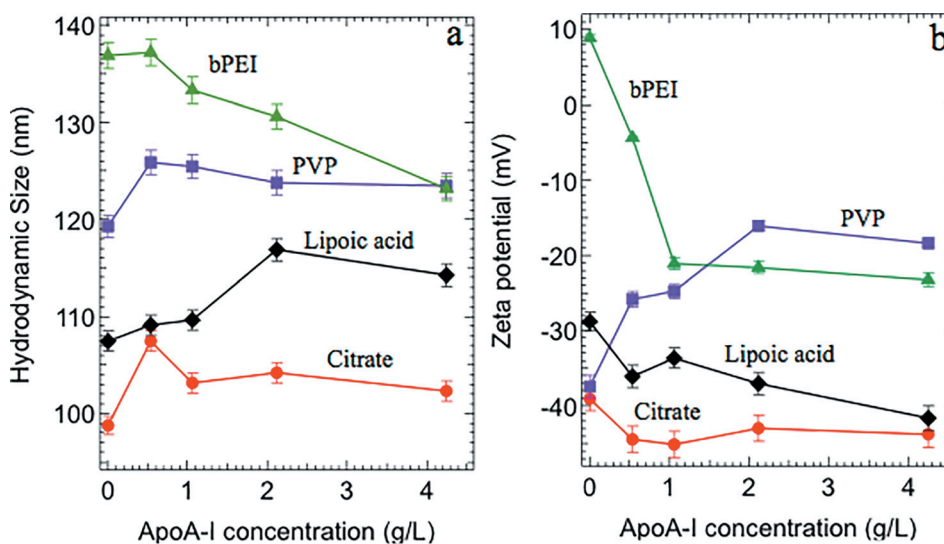

FIG. 2. (a) Hydrodynamic size of AgNPs was found to change with increasing ApoA-I concentrations with saturation >2 g/l for AgNP-PVP, citrate, and lipoic acid coatings. AgNP-bPEI, however, did not show such saturation. (b) The zeta potential measurements showed clear changes indicating the displacement of surface coatings by ApoA-I. All surface coatings showed saturation in zeta potential changes >2 g/l excepting AgNP-lipoic acid. Based on (a) and (b), it could be inferred that AgNP-bPEI and AgNP-lipoic acid do not show saturation in protein adsorption even at high ApoA-I concentrations. It should be noted that the physiological concentration of ApoA-I is 1.3–1.5 g/l.

higher affinity for AgNP surface and ultimately replaced bPEI on AgNP surface. The surface potential of AgNP-PVP decreased with increasing concentration of Apo-A1 similar to bPEI. However, S_{HD} showed a sharp increase with a rapid saturation at relatively low concentration of ApoA-I (<1 g/l). Unlike AgNP-bPEI and AgNP-PVP, a significant increase in S_{HD} for AgNP-lipoic acid was observed only at higher ApoA-I concentrations (>2 g/l). The observed changes in both ζ and S_{HD} were much slower for lipoic acid and can be rationalized in terms of relatively strong Ag-S interactions [binding energy $\sim$217 kJ/mol (Ref. 38)] between sulfur in lipoic acid and the surface of AgNPs. Interestingly, AgNP-citrate showed relatively smaller changes in S_{HD} and ζ compared to other surface coatings. Nevertheless, in all cases, the increase in S_{HD} did not indicate the formation of AgNP gates unlike in the dehydrated state (cf. Figs. S1–S4, Ref. 43). We found that the changes in S_{HD} and ζ saturated above 2 g/l for all surface coatings, except bPEI and lipoic acid. While S_{HD} for AgNP-lipoic acid appears saturated, its ζ did not suggesting that protein adsorption did not saturate. When the average time between consecutive collisions (τ_c) of ApoA-I with AgNPs is greater than ApoA-I configurational relaxation time (τ_R), there is sufficient time for ApoA-I to unfold on AgNP surface and thus could form a disorganized corona. This condition ($\tau_c > \tau_R$) occurs at low ApoA-I concentrations (<2 g/l) for AgNP-PVP and AgNP-citrate. Indeed, disorganized protein aggregates can be clearly observed on AgNP-PVP surface (Fig. S2, Ref. 43). However, at higher $\tau_c \sim \tau_R$, ApoA-I cannot completely unfold due to rapid collisions between ApoA-I and AgNPs. This results in a densely packed corona where ApoA-I retains much of its secondary structure. Based on the results described in Fig. 2, it may be expected that the corona layer present directly on the AgNP surface is densely packed >2 g/l for all cases, except bPEI and lipoic acid, and thus saturates further changes in S_{HD} and ζ. The collision frequency ($f_c = 1/\tau_c$) of ApoA-I molecules with AgNP surface may be calculated using the Smoluchowski equation[39]

$$f_c = 1/\tau_c = 2\pi DCdN_A, \qquad (1)$$

where D = 120 μm^2 s^{-1} is the room-temperature diffusion coefficient of the ApoA-I (Ref. 40), d = 12.8 nm is the room-temperature hydrodynamic diameter of ApoA-I (Ref. 41) and, $N_A = 6.023 \times 10^{23}$ mol^{-1} is the Avogadro number, and C is ApoA-I concentration at which adsorption saturates. At $C = 2$ g/l, we find that $\tau_c \sim 90$ μs, which is on the same scale as protein unfolding timescales. It should be noted that the value of τ_c derived from the above analysis only provides an estimate for the unfolding timescales. Nevertheless, it could be used to infer that ApoA-I molecules will collide on a timescale of few tens of microseconds at physiological concentrations $\sim$1.3–1.5 g/l, leading to a rapid saturation in adsorption.[42]

It is well known that some proteins change their conformation upon binding to nanoparticle surfaces. Previously, Cukalevski *et al.* studied the conformational changes of ApoA-I on polystyrene (PS NPs) and *N*-isopropylacrylamide-*co-N-tert*-butylacrylamide small sized nanoparticles (<60 nm) with large curvature and different surface charges.[33] They found that plain and negatively charged PS NPs (diameter $\sim$23–24 nm) slightly increased the helical structure of ApoA-I in the range of 2%–15% whereas positively charged PS NPs (diameter $\sim$57 nm) slightly reduced the amount of helical structure by $\sim$10%. A similar study by Li *et al.* on 30 nm negatively charged AgNPs and ApoA-I (Ref. 37) also found reduction of helical content by $\sim$15%–20%. Although these previous reports provide some preliminary understanding of ApoA-I interactions with ENMs, a controlled study with AgNPs of same size but different surface coatings is necessary to understand the influence of surface change. In this study, we used 100 nm AgNPs with different surface coatings to clearly distinguish the effects of surface charges and understand the mechanisms involved in ENM-induced protein unfolding. In our CD studies, we found that ApoA-I exhibited a significant decrease in the helical content by >40% on all 100 nm. ApoA-I unfolding is more pronounced in our case due to the large AgNP size compared to previous studies.[33,37] The CD spectra revealed that the changes in helical content were more prominent for AgNP-bPEI and AgNP-lipoic acid compared to PVP and citrate coatings. Indeed, the helical content of ApoA-I may be completely suppressed for these AgNPs (Fig. 3). These changes were accompanied by a concomitant increase in β-sheet and random chain structures in the following order: AgNP-PVP < AgNP-citrate < AgNP-lipoic acid $\sim$ AgNP-bPEI.

As shown in Fig. 4, we performed CV to develop a mechanistic understanding of surface charge dependent conformational changes observed in CD spectra (Fig. 3). Proteins interact with ENM surfaces through intramolecular bonds, ionic bonds, and charge transfer.[24,26] A stabilizing charge may be transferred between proteins and ENM surface depending upon their electronic energy levels, and the adsorbed proteins may undergo various conformational changes during the electron exchange process. Charge transfer processes and the relative differences between electronic energy levels of protein and ENM surface could be ascertained through peaks in current (i.e., charge flow) during a CV scan.[18,39]

In the CV scan of AgNPs without ApoA-I [dashed lines in Fig. 4(a)], we did not observe any peaks for all four surface coatings. The addition of ApoA-I to the electrolyte resulted in a change in voltammetric responses with the appearance of a new peak [blue arrows in Fig. 4(a)], which in turn increased the current considerably. This new peak cannot be attributed to desorption of adsorbed hydrogen [which is known to occur $\sim$990 mV versus Ag/AgCl electrode[39] as the peak appeared at appreciably low potentials <350 mV for all the coatings. We attribute this peak to stabilizing electron transfer between ApoA-I and AgNP surface. The electron transfer occurs only when the electronic energy levels of ApoA-I are in the vicinity of AgNPs energy levels. The so-called Fermi energy (E_F) or the chemical potential of AgNPs (that serve as the working electrode in our CV
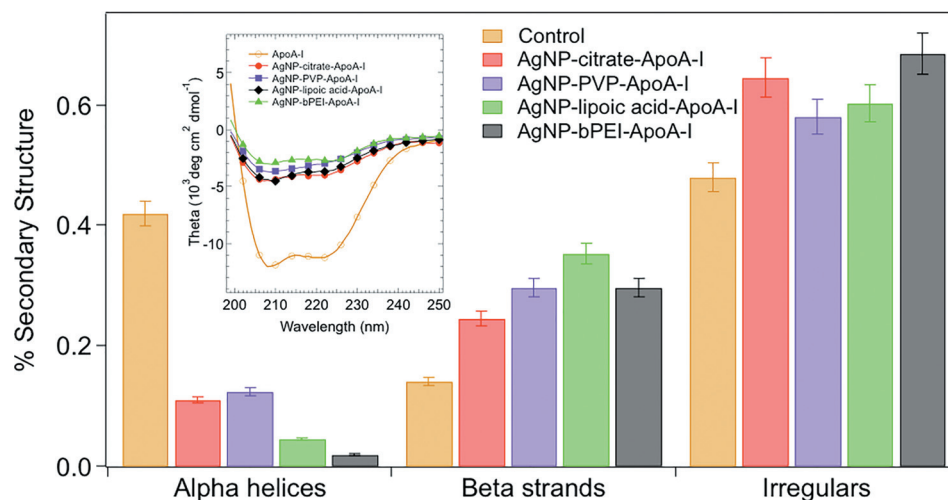
FIG. 3. Circular dichroism spectra for ApoA-I incubated with AgNPs (shown in the inset) of different surface coatings showed marked decrease in helical content with concomitant increase in beta sheets and irregular structures.

measurements) is decreased (/increased) when the voltage in a CV scan is increased (/decreased). An electron transfer occurs when the energy levels of ApoA-I match the altered E_F of AgNPs at a particular voltage in the CV scan. This peak voltage for electron transfer was found to be much lower for AgNP-bPEI and AgNP-lipoic acid ($\sim$60 mV) compared to AgNP-citrate and AgNP-PVP ($\sim$300 mV) suggesting that the surface coatings have considerable influence of electron transfer reactions between ApoA-I and AgNPs [Fig. 4(a)]. The surface coatings have different electronic nature relative to each other and may lead to charge transfer peak at different potentials. The electrochemical charge transfer (Q) can be quantified by calculating the area enclosed by CV curves [Fig. 4(a)]. We found that all the AgNPs showed an increase in Q with increasing ApoA-I concentration concurring with our hypothesis that the observed peak arises from electron transfer between ApoA-I and AgNPs. The normalized areal charge
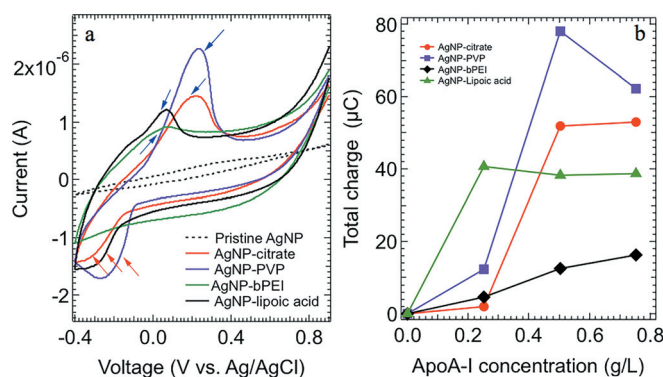
density (Q/cm^2) at higher ApoA-I concentrations showed the following trend: AgNP-PVP > AgNP-citrate > AgNP-lipoic acid > AgNP-bPEI. This trend appeared to match the changes in CD spectra described in Fig. 3.

An interesting feature in the CV scans was the presence of an irreversible charge transfer peak for AgNP-bPEI. For bPEI coating, a peak was observed only when the voltage was increasing in the CV scan indicative of irreversible charge transfer. On the other hand, CV scans for AgNP-citrate, AgNP-PVP, and AgNP-lipoic acid exhibited an observable valley [see red arrows in Fig. 4(a)] during the reverse voltage sweep suggesting that the observed Q for these coatings does not entirely result from irreversible charge transfer reaction. This reversible peak may possibly be attributed to the formation of hydrogen bonds between ApoA-I and surface coatings (PVP, citrate, and lipoic acid). Given that bPEI showed completely irreversible stabilizing charge transfer, we expect greater conformational changes in ApoA-I. In other words, the loss of ApoA-I secondary structure on bPEI coated AgNPs precludes reversibility of charge transfer. Such an observation suggests concurs with the CD spectra, which showed complete loss of α-helical content in bPEI coatings. It could be expected that the disruption of stabilizing hydrophobic interactions in the interior of the protein results in an irreversible charge transfer and ensue in ApoA-I structural relaxation on AgNP-bPEI. On the other hand, AgNP-PVP and AgNP-citrate facilitate hydrogen bond formation with substantial retention of the helical content. Returning to Fig. 3, the loss in α-helical content of ApoA-I on AgNP-lipoic acid cannot be explained based on charge transfer. It is possible that the ApoA-I molecule unfolds on AgNP-lipoic acid surface to increase its interaction with AgNP surface in order to break strong Ag-S interactions in AgNP-lipoic acid.

We assessed the ability of AgNPs with and without ApoA-I corona to generate intracellular ROS by RAW 264.7 macrophages after 1 h exposure using DCF fluorescence
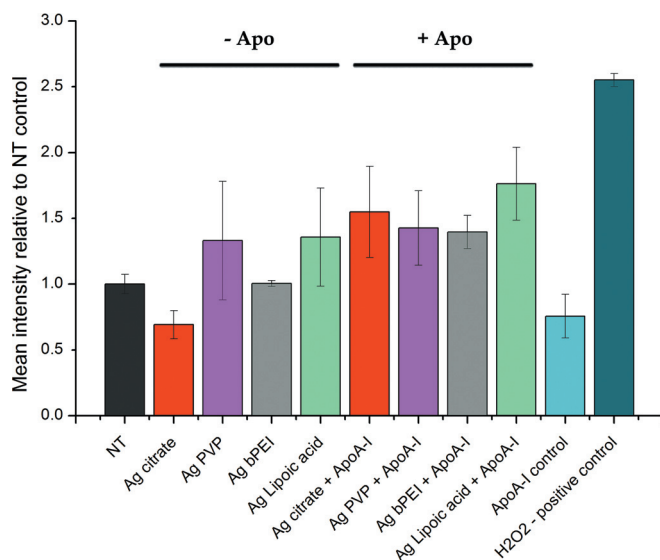

FIG. 4. (a) Cyclic voltammetry scans showed the appearance of a peak (blue arrows) for AgNP electrodes in ApoA-I electrolyte suggesting the presence of charge-transfer stabilizing interactions. The peak for AgNP-bPEI occurred only in the forward scan (going from −0.4 to 0.8 V) indicating irreversible charge transfer. A valley (red arrows), representative of reversible charge transfer, was observed for other surface coatings on the reverse scan (0.8 to −0.4 V). (b) The total charge enclosed by the CV curves in (a) displayed clear increasing trends with ApoA-I concentration confirming that the charge-transfer occurs due to interactions between ApoA-I and AgNPs.

FIG. 5. DCF assay was used to evaluate the ability of AgNPs with (+Apo) and without (−Apo) ApoA-I corona to generate ROS. AgNP-bPEI-ApoA-I displayed significant increase in ROS generation compared to AgNP-bPEI while the response to AgNP-lipoic acid-ApoA-I was significantly higher than the control. These changes may be attributed the protein unfolding observed in AgNP-bPEI and AgNP-lipoic acid (cf. Fig. 3).

assay. As shown in Fig. 5, we did not observe any significant changes (relative to control) in ROS generation for pristine AgNPs without ApoA-I corona irrespective of their surface coatings. We found that the addition of ApoA-I corona led to significant changes in AgNP-lipoic acid-ApoA-I and AgNP-bPEI-ApoA-I relative to the control. However, only AgNP-bPEI-ApoA-I was significantly different from AgNP-bPEI. Based on our CD and CV results, we attribute these changes to the adsorption and unfolding of ApoA-I on AgNP-bPEI and AgNP-lipoic acid. Additionally, in case of AgNP-bPEI, ApoA-I corona resulted in an increased surface charge (accompanied by a change from positive to negative sign) and better stability [cf. Fig. 2(b)] that could have also been a contributing factor to the observed increase in ROS generation. Despite these changes in ROS generation, we did not observe any significant differences in the cytotoxicity of AgNPs before and after ApoA-I adsorption (Fig. S5, Ref. 43). Based on this result (Fig. S5, Ref. 43), changes in AgNP dissolution or uptake upon the addition of ApoA-I corona could be ruled out as possible cause for the observed differences in ROS generation.

IV. CONCLUSIONS

In summary, our dynamic and electrophoretic light scattering studies showed that ApoA-I displaces surface coatings such as citrate, PVP, and bPEI even at low concentrations (<2 g/l). In case of AgNP-lipoic acid, strong Ag-S interactions inhibit ApoA-I adsorption for concentrations below 2 g/l. Circular dichroism studies showed a significant decrease in α-helical content for all surface coatings with the complete disappearance of α-helices for AgNP-bPEI and AgNP-lipoic acid. The changes in secondary structure concur with the

observed charge transfer, measured using cyclic voltammetry, between ApoA-I and AgNPs. The unfolding of ApoA-I on AgNP-lipoic acid cannot be completely explained in terms of charge transfer. It is plausible that ApoA-I unfolds on the surface to lower its free energy and thereby break strong Ag-S interactions in AgNP-lipoic acid. Finally, we found a significant increase in the ability of ApoA-I coated AgNP-bPEI and AgNP-lipoic acid to generate reactive oxygen species, which can be attributed to changes in surface charge and the unfolding of ApoA-I.

[1]M. L. Etheridge, S. A. Campbell, A. G. Erdman, C. L. Haynes, S. M. Wolf, and J. McCullough, Nanomed.: Nanotechnol., Biol., Med. **9**, 1 (2013).
[2]R. Juliano, Nat. Rev. Drug Discovery **12**, 171 (2013).
[3]K. Riehemann, S. W. Schneider, T. A. Luger, B. Godin, M. Ferrari, and H. Fuchs, Angew. Chem., Int. Ed. Engl. **48**, 872 (2009).
[4]V. Wagner, A. Dullaart, A.-K. Bock, and A. Zweck, Nat. Biotechnol. **24**, 1211 (2006).
[5]D. Dutta, *et al.*, Toxicol. Sci. **100**, 303 (2007).
[6]T. Cedervall, I. Lynch, S. Lindman, T. Berggård, E. Thulin, H. Nilsson, K. A. Dawson, and S. Linse, Proc. Natl. Acad. Sci. U. S. A. **104**, 2050 (2007).
[7]A. Lesniak, F. Fenaroli, M. P. Monopoli, C. Åberg, K. A. Dawson, and A. Salvati, ACS Nano **6**, 5845 (2012).
[8]I. Lynch and K. A. Dawson, Nano Today **3**, 40 (2008).
[9]I. Lynch, A. Salvati, and K. A. Dawson, Nat. Nanotechnol. **4**, 546 (2009).
[10]M. P. Monopoli, D. Walczyk, A. Campbell, G. Elia, I. Lynch, F. Baldelli Bombelli, and K. A. Dawson, J. Am. Chem. Soc. **133**, 2525 (2011).
[11]S. Tenzer *et al.*, Nat. Nanotechnol. **8**, 772 (2013).
[12]A. Verma and F. Stellacci, Small **6**, 12 (2010).
[13]C. Corbo, R. Molinaro, A. Parodi, N. E. Toledano Furman, F. Salvatore, and E. Tasciotti, Nanomedicine **11**, 81 (2016).
[14]C. J. Murphy *et al.*, ACS Cent. Sci. **1**, 117 (2015).
[15]C. D. Walkey, J. B. Olsen, H. Guo, A. Emili, and W. C. W. Chan, J. Am. Chem. Soc. **134**, 2139 (2012).
[16]M. P. Monopoli, A. S. Pitek, I. Lynch, and K. A. Dawson, Nanomater. Interfaces Bio.: Methods Protocols **1025**, 137 (2013).
[17]A. Marucco, I. Fenoglio, F. Turci, and B. Fubini, J. Phys.: Conf. Ser. **429**, 012014 (2013).
[18]B. Sengupta *et al.*, RSC Adv. **5**, 82395 (2015).
[19]J. H. Shannahan, J. M. Brown, R. Chen, P. C. Ke, X. Lai, S. Mitra, and F. A. Witzmann Small **9**, 2171 (2013).
[20]J. H. Shannahan, X. Lai, P. C. Ke, R. Podila, J. M. Brown, and F. A. Witzmann, PLoS ONE **8**, e74001 (2013).
[21]R. Podila, R. Chen, P. C. Ke, J. M. Brown, and A. M. Rao, Appl. Phys. Lett. **101**, 263701 (2012).
[22]R. A. Sperling and W. J. Parak, Philos. Trans. Ser. A **368**, 1333 (2010).
[23]P. Satzer, F. Svec, G. Sekot, and A. Jungbauer, Eng. Life Sci. **16**, 238 (2016).
[24]W. Norde, Colloids Surf., B **61**, 1 (2008).
[25]I. Nasir, M. Lundqvist, and C. Cabaleiro-Lago, Nanoscale **7**, 17504 (2015).
[26]C. C. Gibson, D. A. Puleo, and R. Bizios, *Biological Interactions on Materials Surfaces* (Springer Science & Business Media 2009).
[27]R. Huang, R. A. G. D. Silva, W. G. Jerome, A. Kontush, M. J. Chapman, L. K. Curtiss, T. J. Hodges, and W. S. Davidson, Nat. Struct. Mol. Biol. **18**, 416 (2011).
[28]Y. Fang, O. Gursky, and D. Atkinson, Biochemistry **42**, 6881 (2003).
[29]D. W. Borhani, J. A. Engler, and C. G. Brouillette, Acta Crystallogr., Sect. D: Biol. Crystallogr. **55**, 1578 (1999).

[30]A. A. Ajees, G. M. Anantharamaiah, V. K. Mishra, M. M. Hussain, and H. M. K. Murthy, Proc. Natl. Acad. Sci. U. S. A. **103**, 2126 (2006).

[31]X. Mei and D. Atkinson, J. Biol. Chem. **286**, 38570 (2011).

[32]W. S. Davidson and T. B. Thompson, J. Biol. Chem. **282**, 22249 (2007).

[33]R. Cukalevski, M. Lundqvist, C. Oslakovic, B. Dahlbäck, S. Linse, and T. Cedervall, Langmuir **27**, 14360 (2011).

[34]C. C. Fleischer and C. K. Payne, J. Phys. Chem. B **118**, 14017 (2014).

[35]N. Durán, C. P. Silveira, M. Durán, and D. S. T. Martinez, J. Nanobiotechnol. **13**, 55 (2015).

[36]J. H. Shannahan, R. Podila, A. A. Aldossari, and H. Emerson, Toxicological Sci. **kfu217**, 1 (2014).

[37]R. Li, R. Chen, P. Chen, Y. Wen, P. C. Ke, and S. S. Cho, J. Phys. Chem. B **117**, 13451 (2013).

[38]A. Longo, M. Palomba, S. De Nicola, and G. Carotenuto, Polymers **3**, 1794 (2011).

[39]D. R. Jackson, S. Omanovic, and S. G. Roscoe, Langmuir **16**, 5449 (2000).

[40]N. A. Ramella, O. J. Rimoldi, E. D. Prieto, G. R. Schinella, S. A. Sanchez, M. S. Jaureguiberry, M. E. Vela, S. T. Ferreira, and M. A. Tricerri, PLoS ONE **6**, e22532 (2011).

[41]H. J. Schönfeld, D. Roessner, and J. Seelig, J. Phys. Chem. B **120**, 1228 (2016).

[42]A. Leino, O. Impivaara, M. Kaitsaari, and J. Järvisalo, Clin. Chem. **41**, 1633 (1995).

[43]See supplementary material at http://dx.doi.org/10.1116/1.4977064 for more transmission electron micrographs and cytotoxicity data.